$$\frac{1}{N-1}f''-Rf'+\frac{N}{1-N}w'+\frac{Gr}{\mathrm{Re}}\theta+\frac{Gc}{\mathrm{Re}}\phi-Mf'-A=0 \tag{8}$$

$$\frac{2-N}{m_p{}^2}w''-a_j\frac{1-N}{N}Rw'-(2w+f')=0 \tag{9}$$

$$\theta''-R\,\mathrm{Pr}\,\theta'+\frac{Br}{1-N}\left[f'^2+\frac{N(2-N)}{m_p{}^2}w'^2+2N(w^2-wf')\right]+Du\,\mathrm{Pr}\,\phi''+\mathrm{Pr}\,\beta\theta=0 \tag{10}$$

$$\frac{1}{Sc}\phi''-R\phi'+Sr\theta''-\gamma\phi=0 \tag{11}$$

where primes denote differentiation with respect to η, $Sc=\frac{\nu}{D}$ is the Schmidt number, $\mathrm{Pr}=\frac{\mu c_p}{k_f}$ is the Prandtl number, $R_e=\frac{\rho U_0 h}{\mu}$ is the Reynolds number, $Sr=\frac{DK_T(T-T_1)}{\nu T_m(C_2-C_1)}$ is the Soret number, $Du=\frac{DK_T(C_2-C_1)}{\nu C_s C_p(T_2-T_1)}$ is the Dufour number, $R=\frac{\rho v_0 h}{\mu}$ is the suction/injuction parameter, $N=\frac{k}{\mu+k}$ is coupling number, $Gr=\frac{g\rho^2\beta_T(T_2-T_1)h^3}{\mu^2}$ is temperature Grashof number, $Gc=\frac{g\rho^2\beta_c(C_2-C_1)h^3}{\mu^2}$ is the mass Grashof number, $A=\frac{h^2}{\mu U_0}\frac{dP}{dx}$ is the constant pressure gradient, $m_p{}^2=\frac{h^2k(2\mu+k)}{\gamma(\mu+k)}$ is the micropolar parameter, $a_j=\frac{j}{h^2}$ is the micro-inertial density parameter, $Br=\frac{\mu U_0{}^2}{k_f(T_2-T_1)}$ is the Brinkman number.

Boundary conditions (6) in terms of f , ω, θ and φ become

$$\left.\begin{aligned} f=0,\omega=0,\theta=0,\phi=0 \quad at\ \eta=0\\ f=0,\omega=0,\theta=1,\phi=1, \quad at\ \eta=1\end{aligned}\right\} \tag{12}$$

3. Physical Quantities of Interest

The major physical quantities of interest are the skin friction coefficient C_f, Nusselt number Nu, and Sherwood number Sh, which are defined as

$$C_f = \frac{\tau_w}{\rho u_w^2/2}, \qquad Nu = \frac{xq_w}{k\left(T_w - T_\infty\right)}, \qquad Sh = \frac{xq_m}{D\left(C_w - C_\infty\right)} \tag{14}$$

where surface shear stress, surface heat and mass flux are defined as

$$\tau_w = \left[\left(\mu + k\right)\frac{\partial u}{\partial y} + k\omega\right]_{y=0} \qquad q_w = -k\left(\frac{\partial T}{\partial y}\right)_{y=0}, \qquad q_m = -D\left(\frac{\partial C}{\partial y}\right)_{y=0} \tag{15}$$

Using the non-dimensional variables (8), we get from Eqs. (14) and (15) as

$$\frac{1}{2}C_f \,\mathrm{Re}_x^{1/2} = \left(1 + \frac{K}{2}\right)f'(0), \; \frac{Nu}{\mathrm{Re}_x^{1/2}} = -\theta'(0), \; \frac{Sh}{\mathrm{Re}_x^{1/2}} = -\phi'(0) \tag{16}$$

4. Results and Discussion

In order to insight the physical significance of the pertinent physical parameters characterizes the flow phenomena of an electrically conducting micropolar fluid between two parallel plates are discussed. The numerical solutions are obtained to exhibit the effects of emerging physical parameters on the momentum, angular momentum, temperature and concentration distributions through graphs. Also, the numerical computation of the shear stress, for both the momentum profiles, rate of heat and mass transfer are shown in Table-1.

In the present study, flow of an electrically conducting micropolar fluid between two parallel plates subject to transverse magnetic field in the presence of uniform heat source/sink and first order chemical reaction has been investigated. The aim of the investigation is to bring out the effects of additional parameters introduced such as magnetic parameter (M), heat generation / absorption (β) parameter and the destructive / generative chemical reaction (γ) besides the other parameters characterizes the flow phenomena. For the verification the present result is compared with the result of Srinivasacharya and Mekonnen [23] in a particular case.

Figs.2 and 3 illustrate the effect of magnetic parameter on the flow phenomena in the absence of heat source and chemical reaction and the presence of other physical parameters and $N > 1$. In the absence of M (M=0) present result compared with the result of Srinivasacharya and Mekonnen [23] and found that the present result is in good agreement. It is interesting to note that an increase in magnetic parameter enhances the velocity profile at all points in the velocity boundary layer. Also, near the first plate ($\eta < 0.2$), microrotation profile increases as magnetic

parameter increases whereas reverse effect is encountered after that ($\eta > 0.2$) i.e. an increase in magnetic parameter micorotatin profile decelerates.

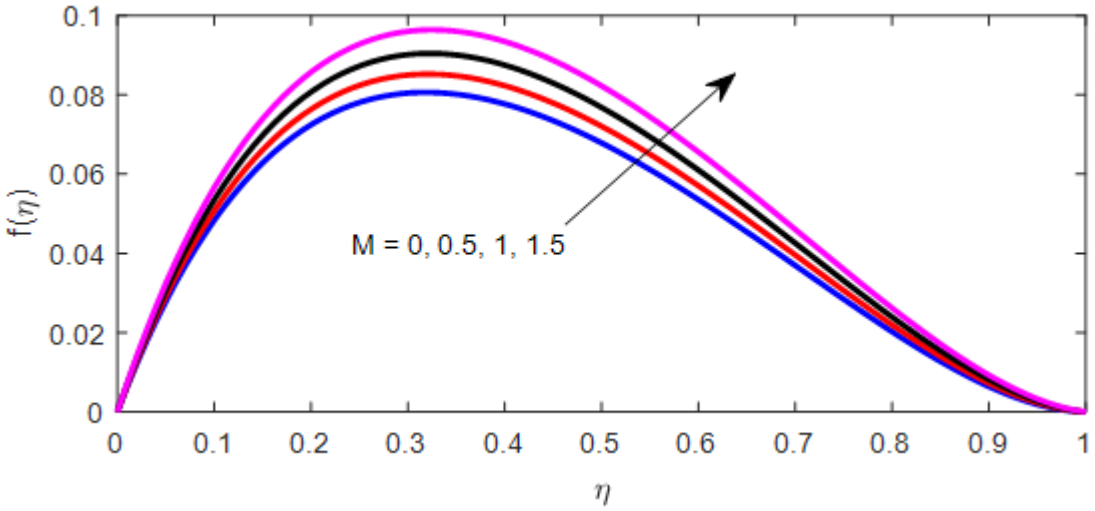

Fig.2. Effect of M on velocity profiles for $N = 2.5$ and $R = 2, Pr = 0.71, Gr = 0.2$ $, Gc = 2,$ $Sc = 2, \gamma = 0, Re = 1, a = 1, aj = 0.001, mp = 1, Br = 1; Du = 1; Sr = 0.2; \beta = 0$

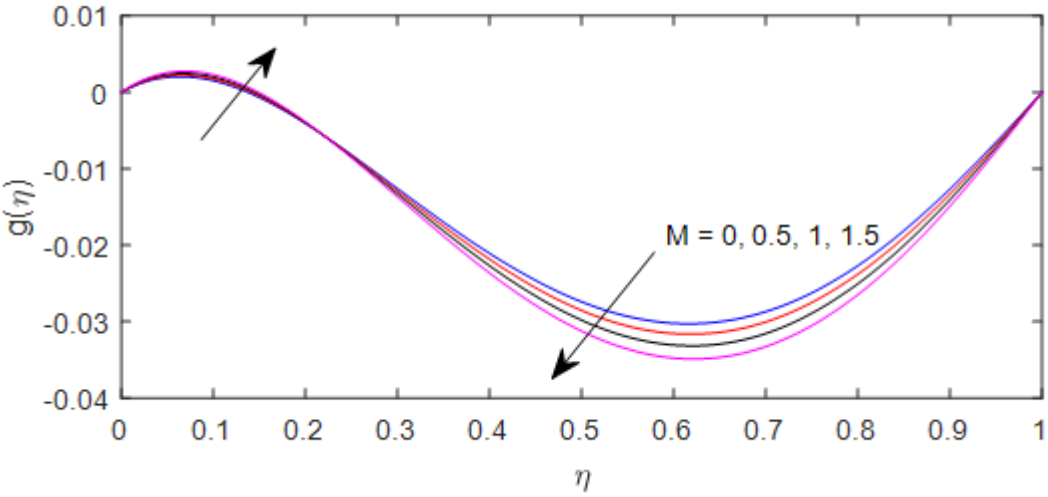

Fig.3. Effect of M on microrotation profiles for $N = 2.5$ and $R = 2, Pr = 0.71, Gr = 0.2$ $, Gc = 2,$ $Sc = 2, \gamma = 0, Re = 1, a = 1, aj = 0.001, mp = 1, Br = 1; Du = 1; Sr = 0.2; \beta = 0$

Figs. 4 and 5 exhibit the effect of magnetic parameter on velocity and microrotation profiles respectively for $N < 1$. It is observed that in both the profile the effect is reverse as that of Figs.2 and 3. The velocity profile retards as magnetic parameter increases. It is due to the Lorentz force which is a resistive force generates due to the interaction of conducting fluid and magnetic field, retards the velocity profile. It is also remarked that the microrotation profile has opposite characteristics about the middle layer of the channel i.e. ($\eta = 0.5$). The profile decelerates before the region $\eta < 0.5$ and then enhances after that region to meet the inadequate boundary conditions.

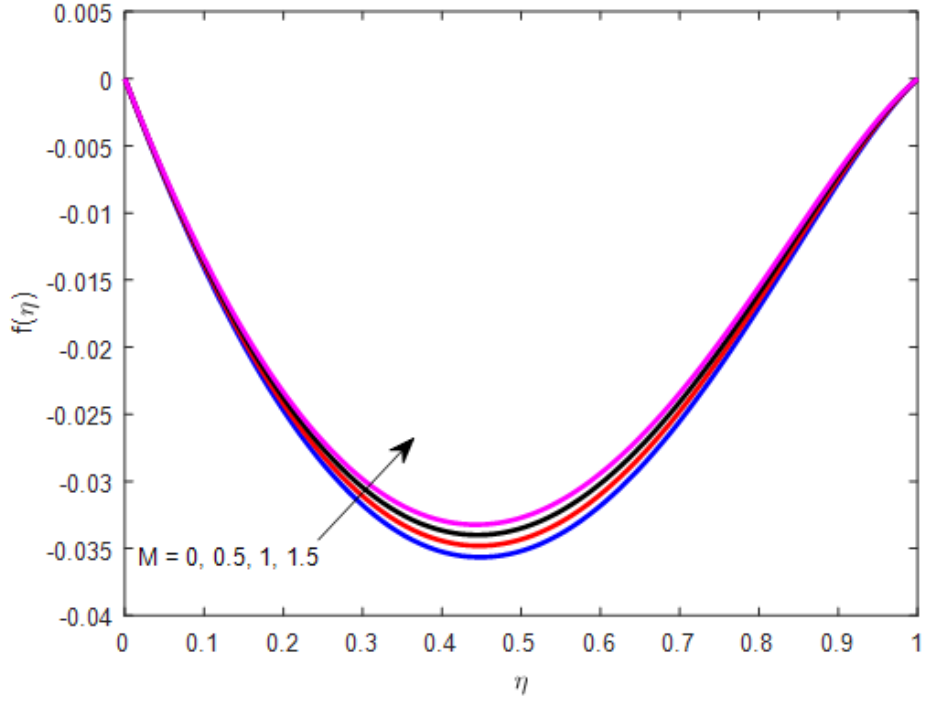

Fig.4. Effect of M on velocity profiles for $N = 0.5$ and $R = 2, Pr = 0.71, Gr = 0.2$ $, Gc = 2,$

$Sc = 2, \gamma = 0, Re = 1, a = 1, aj = 0.001, mp = 1, Br = 1; Du = 1; Sr = 0.2; \beta = 0$

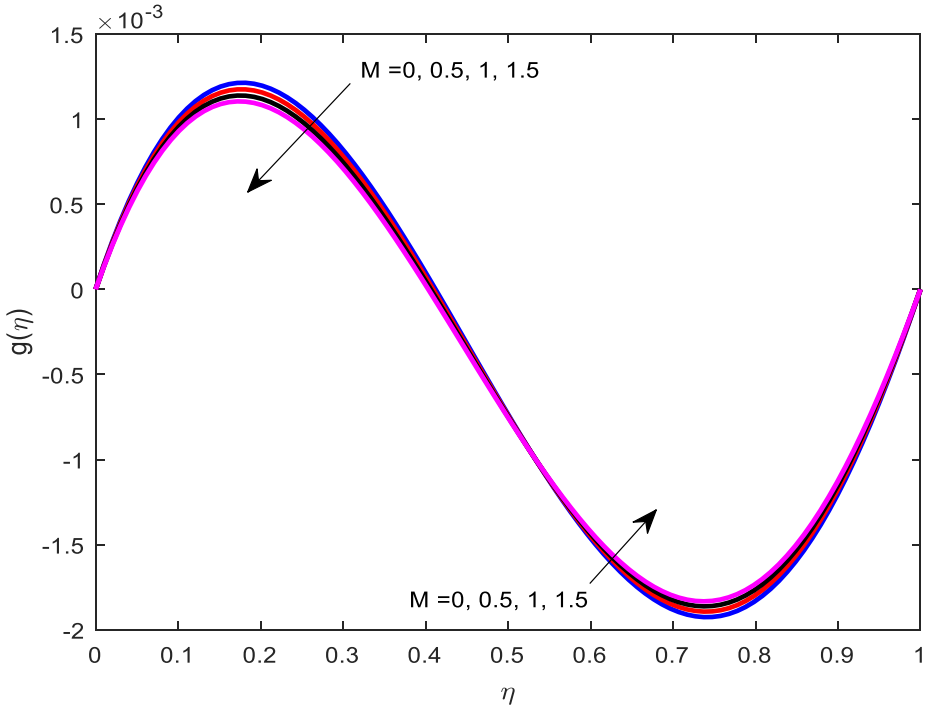

Fig.5 Effect of M on microrotation profiles for $N = 0.5$ and $R = 2, Pr = 0.71, Gr = 0.2$ $, Gc = 2,$

$Sc = 2, \gamma = 0, Re = 1, a = 1, aj = 0.001, mp = 1, Br = 1; Du = 1; Sr = 0.2; \beta = 0$

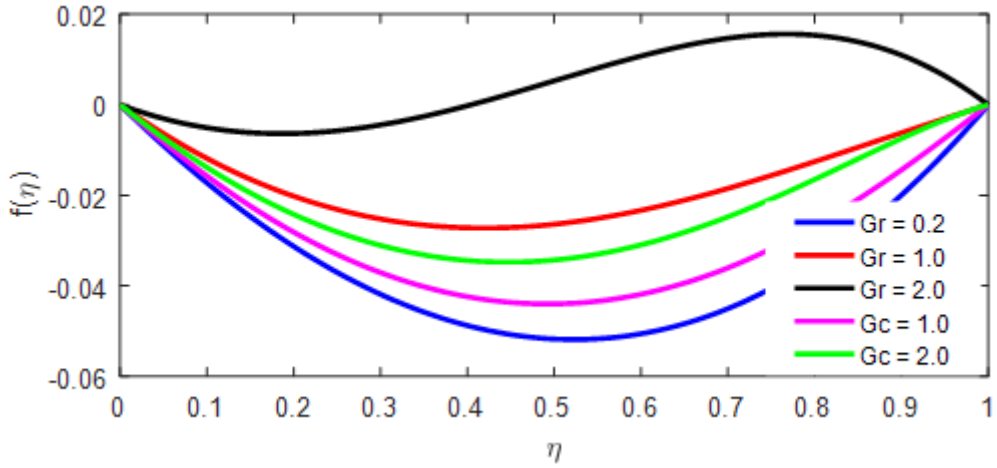

Fig.6. Effect of Gr and Gc on velocity profile for n=0.5 and $R = 2, Pr = 0.71, Sc = 2,\ M = 0.5,$ $\gamma = 0, Re = 1, a = 1, aj = 0.001, mp = 1, Br = 1; Du = 1; Sr = 0.2; \beta = 0$

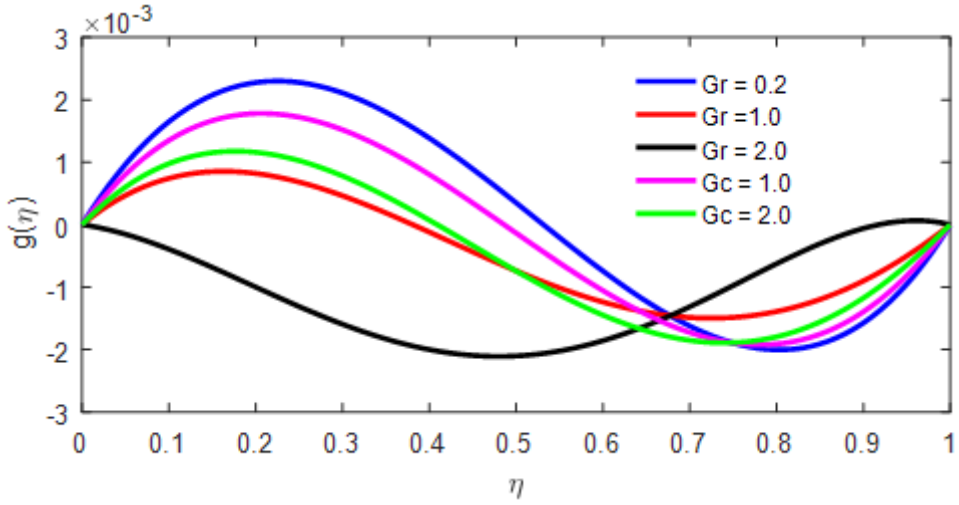

Fig.7. Effect of Gr and Gc on microrotation profile for $N = 0.5$ and $R = 2, Pr = 0.71, Sc = 2,\ M = 0.5,$ $\gamma = 0, Re = 1, a = 1, aj = 0.001, mp = 1, Br = 1; Du = 1; Sr = 0.2; \beta = 0$

The effects of thermal and mass buoyancy parameters on both the velocity and microrotation profiles are exhibited in Figs.6 and 7 in the presence of magnetic and other parameters shown in the caption for $N = 0.5$. It is seen that an increase in thermal buoyancy and mass buoyancy parameter velocity profile increases significantly. For the higher value of thermal buoyancy parameter i.e. $Gr = 2.0$, the velocity becomes maximum (Fig.6). From Fig.7 it is clear that the effect of these buoyant forces behaves adversely as that of velocity in Fig.6 within the region $\eta = 0.65$ and then trend becomes reversed. Hence, it is concluded that higher values of Gr and Gc favours in an increase in the velocity profile.

Fig.8 exhibits the effects of Prandtl number and heat generation (source)/ absorption (sink) parameter on the temperature profile. In case of water ($\Pr = 0.71$), increase in source enhances the

fluid temperature whereas sink opposes it. That is, sink has reverse effect on the temperature profile. Further, it is interesting to note that increase in Prandtl number increases the fluid temperature. In a particular case in the absence of heat source ($\beta = 0$) the present result is in good agreement with that of Srinivasacharya and Mekonnen [23].

Figs. 9 illustrates the effect of Dufour and Soret number on the temperature profile in the presence of magnetic, heat source and other fixed values of the pertinent parameters for $N = 0.5$. It is noteworthy that the increase in Dufour number the fluid temperature increases. The presence of source plays an important role to enhance the temperature of the fluid at all points in the thermal boundary layer.

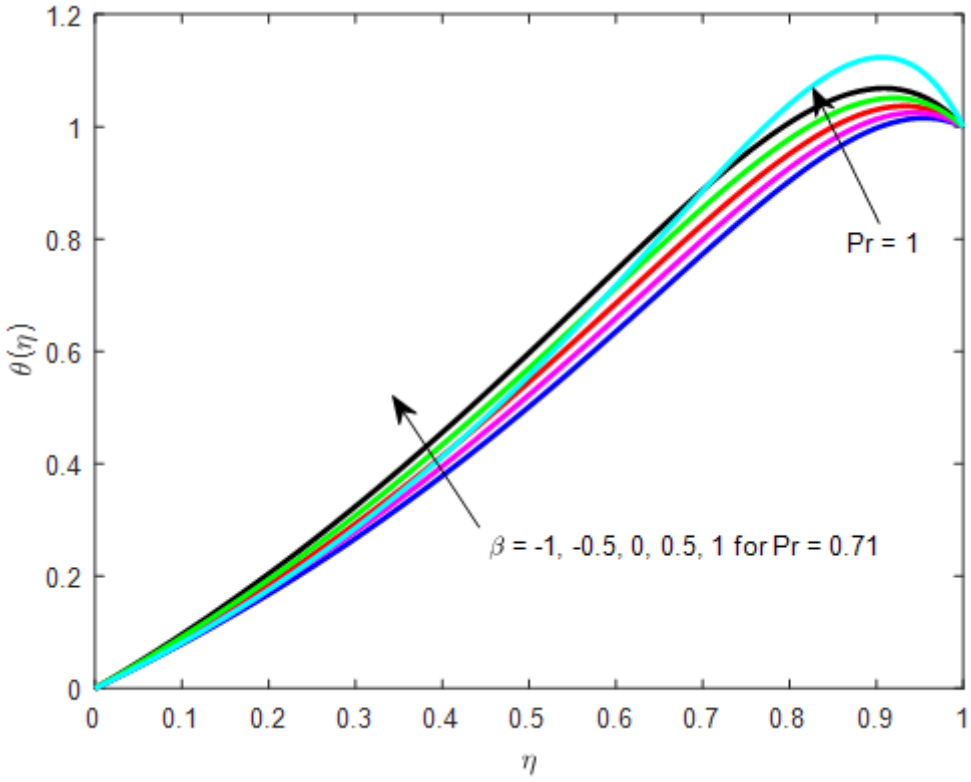

Fig.8. Effect of Pr and β on temperature profile for $N = 0.5$ and

$R = 2, Sc = 2, Gr = 0.2, Gc = 2, M = 0.5, \gamma = 0, Re = 1, a = 1, aj = 0.001, mp = 1, Br = 1; Du = 1; Sr = 0.2$

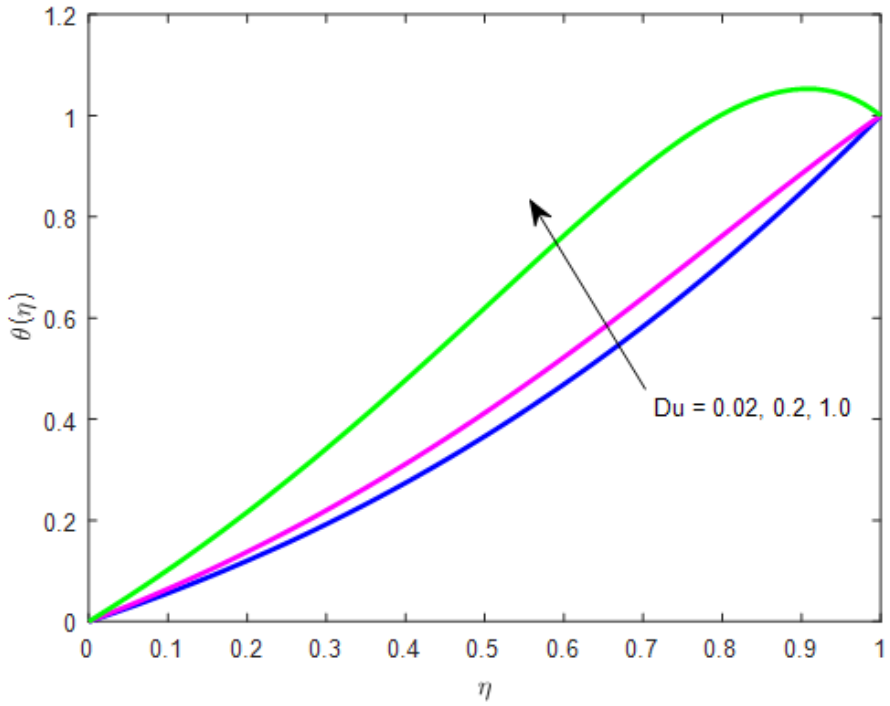

Fig.9 Effect of Du on temperature profile for $N = 0.5$ and

$R = 2, Sc = 2, Gr = 0.2, Pr = 0.71 Gc = 2, M = 0.5, \gamma = 0, Re = 1, a = 1, aj = 0.001, mp = 1, Br = 1; Sr = 0.2; \beta = 1$

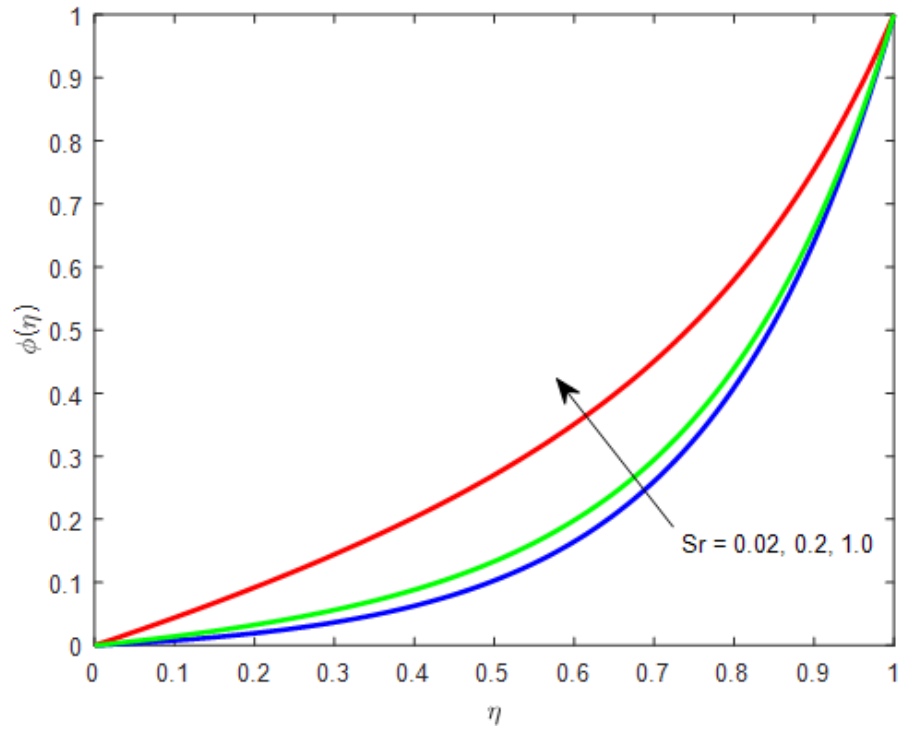

Fig.10 Effect of Sr on Concentration Profile for $N = 0.5$ and

$R = 2, Sc = 2, Gr = 0.2, Pr = 0.71 Gc = 2, M = 0.5, \gamma = 0, Re = 1, a = 1, aj = 0.001, mp = 1, Br = 1; Du = 1; \beta = 1$

Fig.10 presents the effect of Soret on the concentration profile in the absence of chemical reaction parameter. It is observed that the fluid concentration increases as an increase in Soret

number. Presence of heavier species i.e. high value of Schmidt number inclusion with Soret number favours to increase the fluid concentration in its concentration boundary layer.

Fig.11 exhibits the effects of Schmidt number and Chemical reaction on the concentration profile in the presence of magnetic and other fixed values of physical parameters for $N = 0.5$. In the present case we discuss the effect of destructive chemical reaction ($\gamma > 0$), no chemical reaction ($\gamma = 0$) and constructive chemical reaction ($\gamma < 0$). It is clear to note that higher value of chemical reaction i.e. in case of destructive chemical reaction the concentration of the fluid decelerates where as in case of constructive the adverse effect is observed. Also in the absence of chemical reaction the fluid concentration becomes linear. Further the heavier species also decelerates the fluid concentration at all points in the concentration boundary layer.

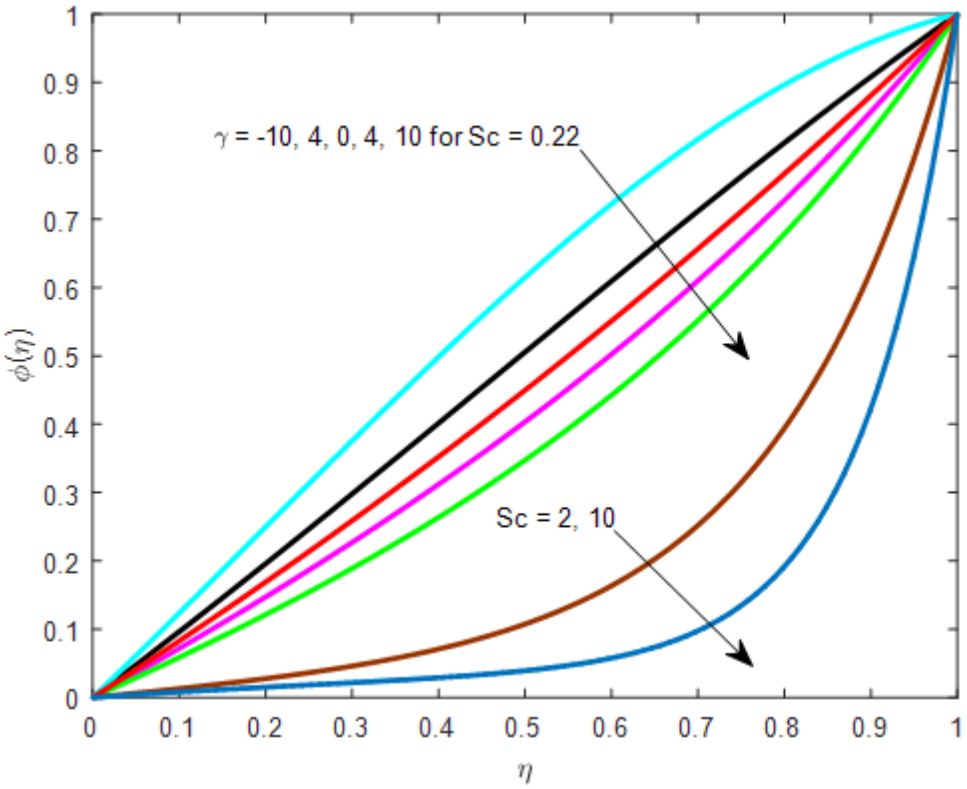

Fig.10. Effect of Sc and γ on Concentration Profile for $N = 0.5$ and

$R = 2, Sc = 2, Gr = 0.2, Pr = 0.71, Gc = 2, M = 0.5, Re = 1, a = 1, aj = 0.001, mp = 1, Br = 1; Du = 1; \beta = 1$

Tab 1. Skin Friction Coefficient, Nusselt Number and Sherwood Number for

$R = 2, Sc = 2, Pr = 0.71, Re = 1, a = 1, aj = 0.001, mp = 1, Br = 1, Du = 1$

M	N	Gr	Gc	β	γ	$f'(0)$	$-\theta'(0)$	$-\phi'(0)$
0	0.5	0.2	2	0	0	-0.157892	0.8208708	0.1562794
0.5	0.5	0.2	2	0	0	-0.155528	0.82056	0.1563524
0.5	2.5	0.2	2	0	0	0.6699169	0.7885034	0.1667105

0.5	0.5	2	2	0	0	-0.038694	0.8153244	0.158287
0.5	0.5	0.2	3	0	0	-0.13738	0.818349	0.1568992
0.5	0.5	0.2	2	-1	0	-0.154896	0.7490826	0.1555779
0.5	0.5	0.2	2	1	0	-0.156302	0.905053	0.1570137
0.5	0.5	0.2	2	1	-1	-0.150885	0.9070298	0.176388
0.5	0.5	0.2	2	1	1	-0.160339	0.903388	0.1426393

The numerical computations of rate of shear stress i.e. skin friction coefficient, rate of heat and mass transfer are obtained and presented in Table-1 for different values of the pertinent parameters and fixed values of other parameters characterizes in the flow phenomena. It is observed that the increasing value of magnetic parameter, thermal and solutal buoyancy decreases the skin friction in magnitude whereas an increase in material parameter, N increases the skin friction coefficient. Also all the parameters except heat source and destructive chemical reaction decreases the rate of heat transfer whereas reverse effect is remarked for rate of mass transfer. Further, sink reduces the rate of heat transfer and constructive chemical reaction is desirable to increase the rate of mass transfer.

5. Conclusion

From the above discussion the following conclusions are made:

- An increase in magnetic parameter velocity profile decreases whereas the microrotation profile enhances for N>1 but reverse effect is observed for N<1.
- Velocity becomes maximum for higher values of buoyant forces.
- Both Dufour and Soret enhance the thermal and concentration boundary layer respectively.
- Both chemical reaction and heavier species retards the concentration profile.
- An increase in N decreases the skin friction coefficient and rate of heat transfer whereas the rate of mass transfer increases.

References

1. A.C. Eringen, Theory of micropolar fluids, 1964, J. Math. Mech., vol. 16, pp. 1–18.
2. T. Ariman, M.A. Turk, N.D. Sylvester, Micro continuum fluid mechanics—A review, 1973, Int. J. Eng. Sci., vol. 11, pp. 905–930.

3. T.C. Chiam, R. Deka, U.N. Das, V.M. Soundalgekar, Effects of mass transfer flow past an impulsively started infinite vertical plate with constant heat flux and chemical reaction, 1994, Forsch. Ingenieurwes., vol. 60, pp. 284–287.
4. M. Ahraf, M. A. Kamal, K. S. Syed, Numerical simulation of a micropolar fluid between a porous disc and a non-porous disk, 2009, Journal of Applied Mathematics and Modeling, vol. 33, pp. 1933-1943.
5. M. Ahraf, M. A. Kamal, K. S. Syed, Numerical simulation of flow of micropolar fluids in a channel with a porous wall, 2011, International journal for Numerical Methods in Fluids, vol. 66, pp. 906-918.
6. Dulal Pal, Sukanta Biswas, Influence of Heat sink on Magento-thermal radiative convective oscillatory flow of micropolar fluid in a porous medium with convective boundary condition, 2016, International Journal of Applied and Computational Mathematics.
7. R. Srinivasa Raju, G. Jithender Reddy, J.Anand Rao, M.M. Rashidi and R.S.R. Gorla, Analytical and numerical study of unsteady MHD free convection with heat absorption, 2016, International Journal Thermal Sciences, vol. 107, pp. 303-315.
8. S.R. Mishra, G.C. Dash, P.K. Pattnaik., Flow of heat and mass transfer on MHD free convection in a micropolar fluid with heat source, 2015, Alexandria. Eng. J., vol. 54, no. 3, pp. 681-689.
9. Shariful Alam, T. Islam, M.J. Uddin, Mathematical modelling for heat transfer of a micropolar fluid along a permeable stretching/shrinking wedge with heat generation/absorption, 2016, Mathematical Modelling of Engineering Problems, vol. 3, no. 1, pp. 1-9.
10. S.R. Mishra, G.C. Dash, M. Acharya., Mass and heat transfer effects on MHD flow of a visco-elastic fluid through porous medium with oscillatory suction and heat source, 2013, Int. J. Heat and Mass Transfer., vol. 57, no. 2, pp. 433-438.
11. R.S. Tripathy, S.R. Mishra, G.C. Dash, M.M. Hoque., Numerical analysis of hydromagnetic micropolar fluid along a stretching sheet with non- uniform heat source and chemical reaction, Engineering Science and Technology, An International Journal., 19(2016)1573-1581.
12. L.A. Dombrovsky, S.S. Sazhin., Absorption of thermal radiation in semi-transparent spherical droplet: A simplified model, 2003, International Journal of Heat and fluid Flow, vol. 24, pp. 919-927.
13. J.A. Shercliff, A text book of magnetohydrodynamics, 1965, Pergamon Press, New York, USA.

14. B. Gebhart, Effect of viscous dissipation in natural convection, 1962, J. Fluid Mech., vol. 14, pp. 225-232.
15. M.M. Rahman, Convective flows of micropolar fluids from radiative isothermal porous surfaces with viscous dissipation and Joule heating, 2009, Commun. Nonlinear. Sci. Simulat. vol. 14, pp. 3018-3030.
16. M.D. Ziaul Haque, M.D. Mahmud Alam, M. Ferdows, A. Postelnicu, Micropolar fluid behaviours on steady MHD free convection and mass transfer flow with constant heat and mass fluxes, Joule heating and viscous dissipation, 2012, Journal of King Saud University-engineering Sciences, vol. 24, pp. 71-84.
17. S. Siva Reddy, M.D. Shamshuddin, Heat and mass transfer on the MHD flow of a micropolar fluid in the presence of viscous dissipation and chemical reaction, 2015, Procedia Eng., vol. 127, pp. 885-892.
18. P.K. Rout, S.N. Sahoo, G.C. Dash and S.R. Mishra, Chemical reaction effect on MHD free convection flow in a micropolar fluid, 2016, Alexandria Eng. J., vol. 55, no. 3, pp. 2967-2973.
19. M.M. Rahman, A. Aziz, M.A. Al-Lawatia, Heat transfer in micropolar fluid along an inclined permeable plate with variable fluid properties, 2010, Int. J. Thermal. Sci., vol. 49, no. 6, pp. 993-1002.
20. D. Ajaz Ahmad, K. Elangovan., Effect of inclined magnetic field on the oscillatory flow of micropolar fluid in a porous micro-channel under the action of alternating electric field, 2016, World Journal of Engineering and Technology, vol. 2, no. 6, pp. 125-145.
21. A.R.M. Kasim Aurangzaib, N.F. Mohammad, S. Shafie, Unsteady MHD mixed convection flow of a micropolar fluid along an inclined stretching plate, 2013, Heat Transfer Asian Research, vol. 42, no. 2, pp. 89-99.
22. D. Srinivasacharya, K. Hima bindu, Entropy generation in a micropolar fluid flow through an inclined channel, 2016, Alexandria Engineering Journal, vol. 55, pp. 973-982.
23. D. Srinivasacharya, ·Mekonnen Shiferaw, Flow of micropolar fluid between parallel plates with Soret and Dufour effects, 2014, Arab J Sci Eng., vol. 39, pp. 5085–5093.
24. A.K. Dash, B.P. Acharya, Mathematical model for entropy generation analysis of MHD micropolar fluid flow: A numerical study, 2017, JCBPS; section-C, vol. 7, no. 2, pp. 85-300.

Nomenclature

C Fluid concentration

D Coefficient of the mass diffusivity

Pr	Prandtl number
g	Acceleration due to gravity
M	Magnetic parameter
k	Material parameter
C_p	Specific molecular diffusivity

Greek symbols

Sc	Schmidt number
$\theta(\eta)$	Dimensionless temperature
T	Fluid temperature
μ	Dynamic viscosity
T_∞	Fluid temperature at infinity
δ	Solutal buoyancy parameter
B_0	Magnetic flux density
α	Thermal diffusivity
Sh	Sherwood number
σ	Electrical conductivity
k_f	Thermal conductivity
λ	Thermal buoyancy or mixed convection parameter
Nu	Nusselt number
ρ	Density of the fluid
u, v	Velocity components along x- and y-direction
κ	Vortex viscosity or microrotation viscosity
j	Micro-inertia density
C_w	Stretching sheet concentration
Ec	Eckert number
T_w	Stretching sheet temperature
x, y	Coordinates
γ	Chemical reaction parameter
ν	Kinematic viscosity
C_1	Species concentration at upper plate
β	heat source/sink parameter
ω	Angular Velocity or microrotation vector
$\phi(\eta)$	Non-dimensional concentration parameter